Biomass Conversion and Biorefinery (2024) 14:10289–10304
https://doi.org/10.1007/s13399-022-03133-5

ORIGINAL ARTICLE

Experimental study of quenching behavior of quenchant prepared from gutter oil at different oil bath temperatures

Zongxiu Zhu[1] · Weiyi Zhang[1] · Dewen Zhang[1] · Zhan Gao[1] · Jiqiu Qi[1] · Fuxiang Wei[1] · Qingkun Meng[1] · Yaojian Ren[1] · Lichao Chai[2] · Zhi Sun[1] · Yanwei Sui[1]

Received: 6 May 2022 / Revised: 6 July 2022 / Accepted: 20 July 2022 / Published online: 8 August 2022

Abstract

The reuse of gutter oil has always been a sensitive social issue. In the heat treatment industry, engineers have also been troubled by the need to move away from dependence on petroleum derivatives for cleaner production. While vegetable oils appear to be a viable alternative, the higher cost and poor thermal and oxidative stability limit their use in the heat treatment industry. The use of gutter oil as a quenchant raw material not only makes the quenchant cost effective but also environmentally friendly. In this study, the cooling performance of fatty acid methyl ester prepared from gutter oil was evaluated and compared with soybean oil and mineral oil. Firstly, fatty acid methyl ester was obtained by esterification and transesterification of gutter oil to reduce the free fatty acid content and make it suitable for quenching and heat treatment. The experiments were carried out using an Inconel 600 standard probe according to ISO 9950. The cooling behavior of the quenching media was tested at oil bath temperatures of 40 °C, 60 °C, and 80 °C. Quenching was carried out using AISI 4340 to obtain Vickers microhardness distributions on cross-sections of heat-treated specimens and residual stresses were determined by x-ray diffraction for all test materials. The fatty acid methyl ester used for analysis produced a hardening depth equivalent to that of commercial mineral oil when quenching the AISI 4340 alloy steel. And the test results achieved cooling properties and quenching intensity comparable to mineral oil. This indicates that fatty acid methyl ester prepared from gutter oil has the potential to replace mineral oil.

Keywords Gutter oil · Transesterification · Wetting character · Quenching · Cooling curve · Hardening hardness

1 Introduction

In developing countries, due to the lack of legal constraints and waste recycling infrastructure, many food service industries generate cooking oil and animal fats that are discharged directly into the sewer. In China, some unscrupulous vendors collect waste fats and oils from sewers for processing and purification. They will mix the processed waste fats and oils with ordinary vegetable oils and sell these mixed fats, which are seriously hazardous to human health, at low prices in the market. This mixture of fats and oils is known as gutter oil [1]. These illegally sold gutter oils not only contain excessive levels of bacteria, but also toxic chemical compounds such as polychlorinated biphenyls (PCBs) and dioxins [2]. Even when gutter oil is not placed directly on the table as edible oil, but is used as an animal feed additive, these toxic chemical components are just as likely to contaminate meat and other foods through the food chain [3]. Animal feed additives are more difficult to identify through testing, making it very difficult to prevent gutter oil from re-entering the food industry. Therefore, in addition to increased government enforcement to stop the flow of gutter oil, we should provide a more profitable application for the disposal and recycling of gutter oil. In this way, the probability of gutter oil entering the food industry is reduced. One promising application is the use of gutter oil as a quenchant.

✉ Zhi Sun
sunzhi@cumt.edu.cn

✉ Yanwei Sui
wyds123456@outlook.com

[1] Jiangsu Province Engineering Laboratory of High Efficient Energy Storage Technology and Equipments, School of Materials Science and Physics, China University of Mining and Technology, Xuzhou 221116, People's Republic of China

[2] Nanjing Mattel Thermal Processing Technology CO, LTD, Nanjing 210000, People's Republic of China

Quenching technology is an important part of metal heat treatment process. The technology make workpiece form lower bainite or martensite structure by cooling the hot metal workpiece. The main process of quenching technology is divided into two main stages: heating and cooling. In the heating stage, the workpiece is preheated to the austenitizing temperature (most steel materials austenitizing temperature is between 850–900 °C) and maintained for a period to promote the formation of uniform austenite [4]. The cooling process is usually accomplished by immersing the workpiece in the cooling liquid to dissipate the heat [5]. In the cooling stage, the austenitizing workpiece is cooled to room temperature with a very rapid cooling rate, so that a complete or partial martensitic transformation of the workpiece material takes place [6]. The goal of this process is to obtain workpiece with high hardness, high wear resistance, and low residual stress. To achieve this purpose, the cooling stage must be selected to meet the cooling characteristics of the process needs of excellent quenching medium [7].

There are many fluids that can be used as cooling media for heat treatment [8–11], such as water, brine, mineral oil, and vegetable oil. Quenching using water is the most common quenching process. However, the cooling capacity of water as a quenchant is too strong. Workpieces quenched using water generally produce large residual stresses. Water can only be used for quenching workpieces with simple shapes and precision requirements [12]. So, the precise and complex shaped workpiece quenching mainly use oil-based quenchant. Among these, vegetable oils, especially non-edible ones, have received attention in recent research [13, 14]. Due to their green and non-polluting nature, vegetable oils have the potential to replace petrochemicals [15]. Vegetable oils are often used in research into new composite materials to replace plastic products. Clearly, they also have the potential to replace mineral oils as quenchants.

Vegetable oils have been used as heat treatment quenchers for hundreds of years, with historical records relating to them dating back to the Middle Ages. Meanwhile, vegetable oil as a biomass feedstock has many advantages such as good biodegradability, low biotoxicity, and no environmental pollution [16]. The performance of various vegetable oils as quenching media has been extensively studied [17–19]. In some studies, vegetable oil quenching has achieved better quenching performance compared to mineral oil quenching media [20]. However, at the same time, the high cost of raw materials and the poor oxidation resistance of vegetable oils have limited the use of vegetable oils as quenching media. During long-term use, oxidation and hydrolysis of vegetable oils will gradually lead to changes in their properties [21–23]. To improve the thermal stability of vegetable oils, many methods have been used by industry. E.C. de Souza uses the addition of antioxidants to enhance the thermal stability of vegetable oils [24]. Simencio Otero tested the quenching properties of epoxidized soybeans [25]. Some researchers also have used natural vegetable oils to synthesize fatty acid methyl ester (FAME) as quenchant [26]. However, the above options are costly and do not offer the advantage of being a complete replacement for mineral oil quenching media.

In China, the catering industry produces 50 million tons of waste kitchen grease every year. Due to the lack of a proper recycling mechanism, a large amount of waste grease is discarded in the sewers as gutter oil. Compared to ordinary vegetable oil, gutter oil is a mixture of various vegetable oils and animal fats. The composition of gutter oil is more complex, with more impurities and gutter oil fatty acids in the form of free fatty acids. However, gutter oil is cheaper than vegetable oil and is more suitable for use as a base oil for quenching media.

In the current research on vegetable oil quenching media, most of studies have made fresh vegetable oil as the object of study. In recent years, Prathviraj [19] and Samuel [27] have investigated the potential of waste cooking oil as quenchants. These studies lack documentation of the specific chemical composition of the quenchant. Rare researchers have studied the effect of composition on cooling performance. In addition, these studies did not investigate the effect of different media oil bath temperatures on the cooling performance during quenching. This date is essential for the improvement of quenching media. To fill this research gap, we have investigated the quenching performance of quenching media prepared from gutter oil at different oil bath temperatures. In this study, fatty acid methyl esters were prepared from gutter oil by esterification and transesterification using methanol. The fatty acid methyl esters prepared from gutter oil were also tested for composition. The cooling performance parameters of the fatty acid methyl esters prepared from gutter oil were experimentally tested at different oil bath temperatures. Quenching experiments were carried out using FAME as the quenching medium to test the hardness pattern of FAME-quenched specimens at different oil bath temperatures. The performance differences between this new quenching medium and common soybean oil and mineral oil were also compared. The aim of this study was to find a new way of using gutter oil as an industrial application. By studying the quenching properties and cooling characteristics of fatty acid methyl ester prepared from gutter oil, a new idea for the industrial application of gutter oil is provided.

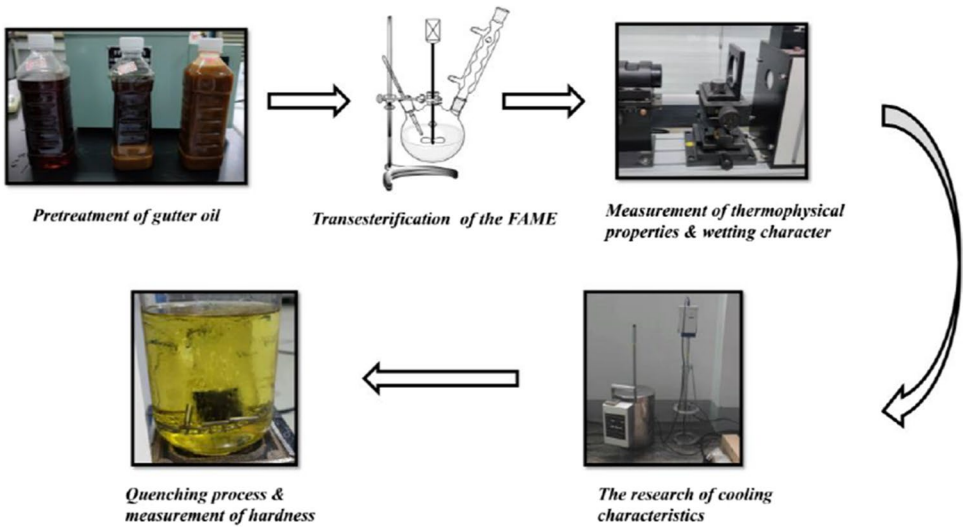

Fig. 1 Sequence of experiments

2 Methodology

The experimental methods and procedures applied in this work are presented in a flow chart approach in Fig. 1. After "2.1 Preparation of quenchants" preparation of fatty acid methyl ester samples, the wettability of the quenching medium on the steel surface was examined for FAME and the control groups (section "2.2 Thermophysical properties and wettability of the quenchant"). The cooling rate of FAME as well as the control groups of soybean oil and mineral oil was tested using a cooling rate test apparatus (section "2.3 The research of cooling characteristics"). The steel samples were then quenched in different quenchants (section "2.4 Quenching process and measurement of hardness"). The microhardness of the specimens was also tested to evaluate the quenching effect under different quenching media conditions.

2.1 Preparation of quenchants

2.1.1 pretreatment of used cooking oil

In this study, fatty acid methyl ester prepared from gutter oil was used as a raw material to investigate its performance as a quenchant. Three quenching agents, fatty acid methyl ester, soybean oil, and mineral oil, were used to compare the differences in quenching performance between different quenchant. Among them, fatty acid methyl ester in this study was prepared from gutter oil. Gutter oil is purchased from kitchen waste oil treatment plants, and its main components are fatty acid triglycerides and free fatty acids. However, gutter oil contains a lot of water and impurities and should not be used directly.

First, the gutter oil is refined and dried. Fifteen grams of activated white clay are added as a filtering agent to each 100 g of oil sample to be treated. The oil was stirred at 300 r/min and heated and held at a temperature of 90 °C for 25 min. The treated oil sample is poured into a Brinell funnel, and the oil is separated from the white clay filtering agent after negative pressure filtration. The filtered oil sample is dried under vacuum and then prepared for use.

2.1.2 Transesterification process of the esterified oil

After pretreatment, the water content and impurity content of the gutter oil are greatly reduced. However, as the treated raw material still contains a high amount of free fatty acids, it cannot be directly processed for transesterification. Therefore, the pretreated used cooking oil samples still need to be further methylated to reduce the free fatty acid content. The acid value of the treated kitchen waste oil was determined using the NaOH titration method to determine the molecular weight of free fatty acids contained in each gram of waste oil. Excess methanol was added in the ratio of alcohol to acid 10:1, and 5% of the oil sample mass of solid acid catalyst HND-8 was added, and the mixture was placed in a magnetic heating stirrer at 250r/min and heated to 70 °C and held for 7 h. The NaOH titration test was performed again, and if the acid value of the oil sample was lower than 2 mg KOH/g, the next step of the transesterification reaction could be performed.

The triglyceride content can be calculated by testing the saponification value of the oil and grease mixture after methanol esterification. An excess of five times the mass of methanol is added as a requirement for the ester exchange reaction to the mixture. NaOH at 2% of the oil sample mass was added to methanol as the reaction catalyst, mixed and dissolved thoroughly, and then added to the oil solution. The mixture was placed in a magnetic heating stirrer at 250 r/min and heated to 65 °C and held for 1 h. After the reaction,

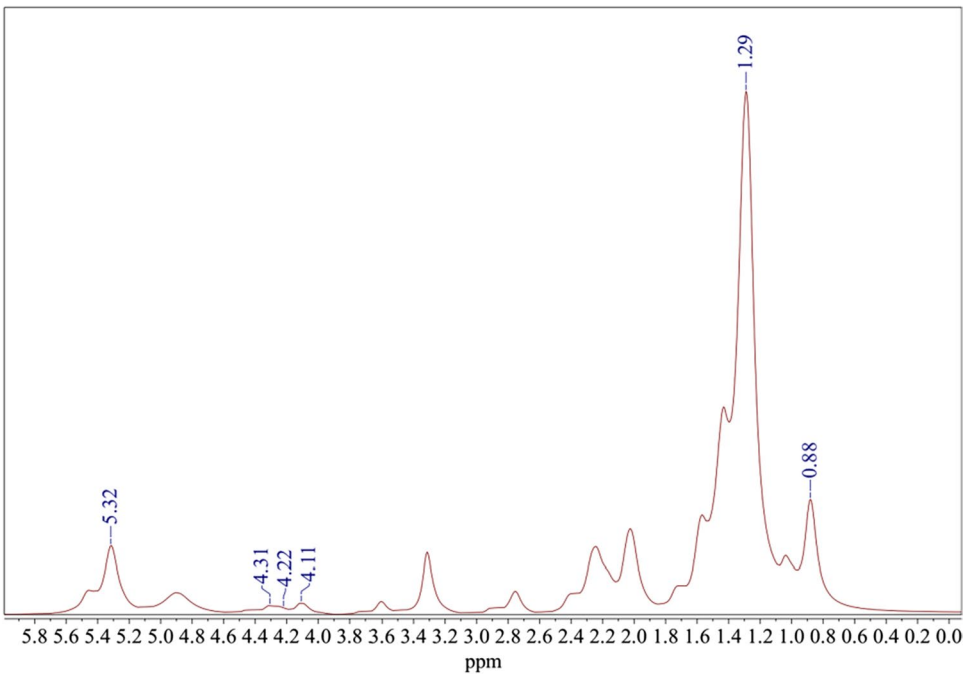

Fig. 2 1H-NMR, spectrum of waste cooking oil

the reaction products were placed in a partition funnel and left for 2 h, which allowed the denser glycerol and methyl ester to be separated into two layers by gravity. The lower glycerol liquid layer was separated and washed twice with distilled water in the remaining fatty acid methyl ester. The water-washed oil sample was dried using a rotary evaporator to remove the remaining water and methanol from the oil sample. The final quenching medium of fatty acid methyl ester was obtained.

2.2 Thermophysical properties and wettability of the quenchant

The kinematic viscosity properties of the three quenching media were tested at 40 °C, 60 °C, and 80 °C using an immersion viscosity cup. The flash point and ignition point temperatures of the three quenching media were also tested in a Cleveland open cup. The wetting characteristics of the quench media were analyzed by measuring the contact angle

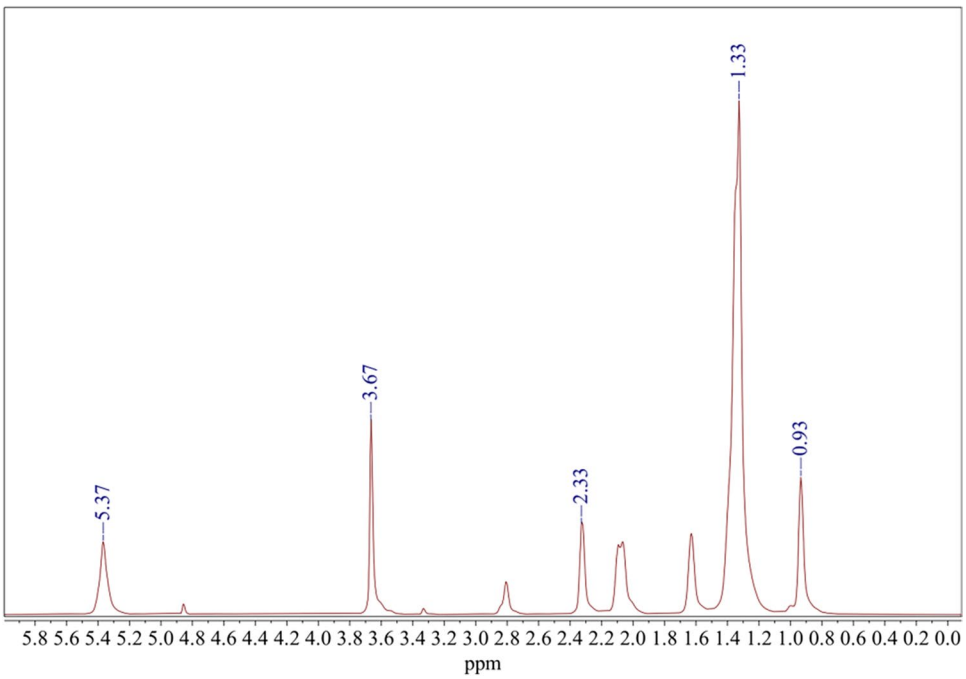

Fig. 3 1H-NMR, spectrum of FAME after transesterification reaction

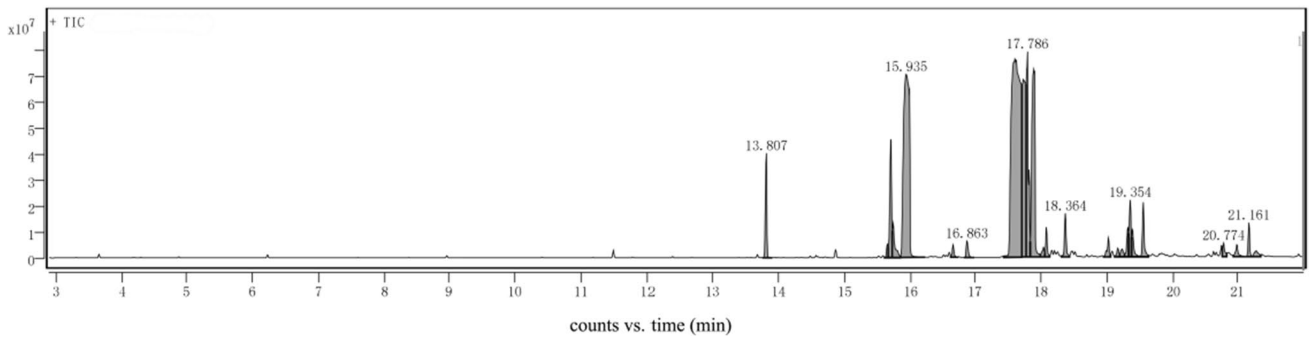

Fig. 4 GC–MS, spectrum of FAME

of the oil droplets on the Inconel 600 substrate. The measurements were performed with the help of a Wetting Angle Tester Type 2021A. The diffusion process of the oil droplets on the substrate was recorded at a recording speed of 200 frames per second (FPS) for a period of 10 s.

2.3 The research of cooling characteristics

The cooling characteristic testing system of quenching oil is designed according to the international standard ISO 9950–1995. The whole test system consists of three main parts: heating furnace, test probe and data collector, and computer control system. Among them, the probe material is made of nickel alloy, and the Inconel 600 standard probe with 12.5 mm diameter and 60 mm length is made. An aperture of 0.5 mm in diameter and 36 mm in depth was drilled in the center of the probe cylinder to accommodate the k-type thermocouple probe, and a hollow steel pipe of 12.5 mm in diameter and 200 mm in length was welded to the rear half of the probe. To simulate quenching conditions, the heated nickel alloy probe is immersed in the quenching medium for cooling, and the k-type thermocouple probe measures the change in probe temperature over time during the quenching process. This is used to determine the cooling capacity of the quenching medium at different cooling stages.

Prior to testing, the probe was heated to austenitization temperature in a resistance tube furnace at 860 °C for 15 min. The thermocouple was connected to a data acquisition system (NI-c-DAQ 9174) with a temperature data measurement acquisition interval of 0.1 s. The heated probe was then immersed without stirring into the prepared quenchant of 1000 mL at 40 °C, 60 °C, and 80 °C, respectively, and cooled. The cooling characteristics of the quenching media were tested at these three temperatures commonly used in industry for quenching media. After the tests, the temperature versus cooling rate and temperature versus time curves were calculated from the measured temperature–time curve variation data.

2.4 Quenching process and measurement of hardness

The AISI 4340 steel was cut into round steel bars of Φ30 × h30mm size and used as specimens for quenching process simulation for quenching tests. For the test, the small steel bar used as the specimen was heated to 860 °C in a muffle furnace and held for 40 min. The purpose of this step is to fully austenitize the bar material. Afterwards, the

Table 1 Fatty acid composition of FAME

Components	Number of components
Methyl tetradecanoate	2.77%
Methyl palmitoleate	5.31%
Methyl palmitate	18.40%
Methyl heptadecanoate	0.95%
Methyl linoleate	33.84%
Methyl oleate	18.34%
Methyl stearate	10.80%
Methyl linolenate	3.95%
Methyl eicosenate	2.67%
Methyl arachidate	1.60%
Lignoceryl erucate	0.53%
methyl behenate	0.84%

Table 2 Thermophysical properties of quenchants

Properties	Mineral oil	Soybean oil	FAME
Density [g/cm^3]	0.88	0.94	0.87
Flash point [°C]	165	345	182
Thermal conductivity [W/m·K]	0.140	0.155	0.160

Table 3 Viscosity of quench oils

Temperature	Mineral oil	SBO	FAME
25 °C	14.16	53.83	16.56
40 °C	9.09	30.29	9.35
60 °C	3.7	21.88	6.103
80 °C	0.68	16.88	4.48

red-hot steel bar specimens are quickly quenched in a beaker containing 2000 ml of quenching medium. A metal mesh was set up in the middle of the beaker to prevent the specimen from touching the bottom of the beaker and affecting the quenching test results. The AISI 4340 steel specimens were tested for quenching in soybean oil, mineral oil, and FAME at 40 °C, 60 °C, and 80 °C oil bath temperatures. The quenched and cooled specimens were cut radially from the center of the bar using a wire cut, and the cut circular section of the bar was ground and polished. Microhardness tests were performed along the radial direction from the center of the cross-section towards the edge of the specimen cross-section. Microhardness tests were performed at 1-mm intervals in the cross-section to obtain the hardness gradient distribution of the specimen cross-section.

X-ray diffraction analysis of the surface of the tested samples at the closest actual production oil bath temperature of 80 °C was performed with a special residual stress diffractometer under Cr-Ka radiation. The stress values were measured by measuring the reflection from the ferrite lattice (211) plane with an x-ray diffraction angle interval of − 45° to 45°.

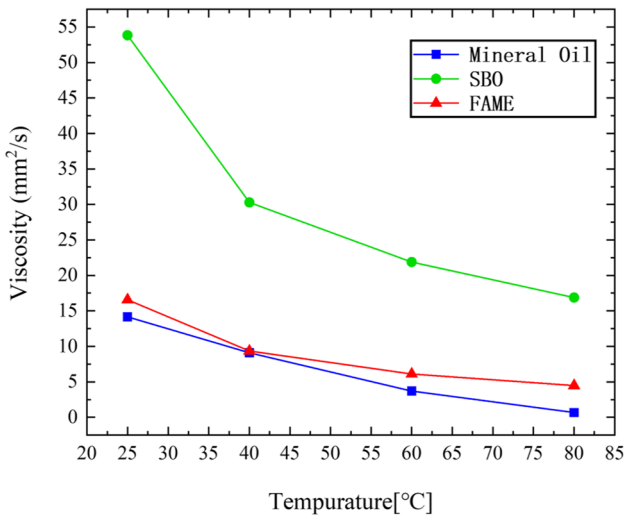

Fig. 5 Viscosity of quench oils

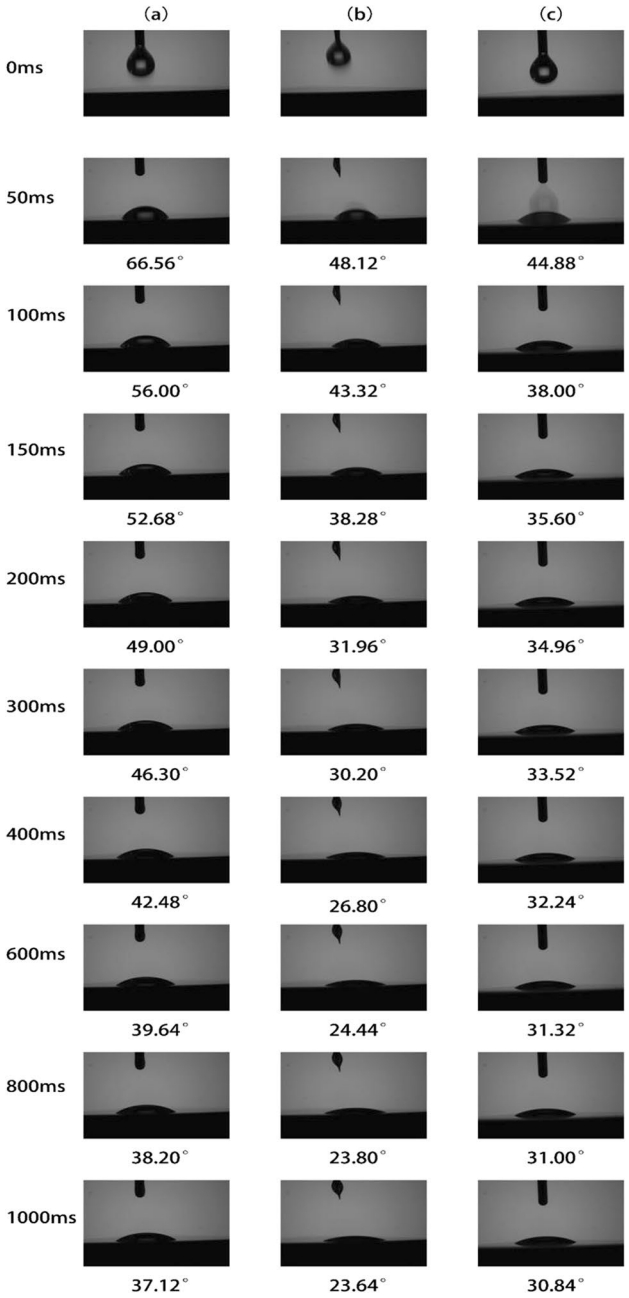

Fig. 6 The contact angle relaxation of **a** soybean oil, **b** mineral oils, **c** FAME on Inconel 600 substrate

3 Results and discussion

3.1 Result of the transesterification process

Nuclear magnetic resonance hydrogen spectroscopy (H-NMR) analysis was performed on the fatty acid methyl esters from the ester exchange treatment to determine the degree of completeness of the ester exchange reaction carried out. And gas chromatography–mass spectrometry

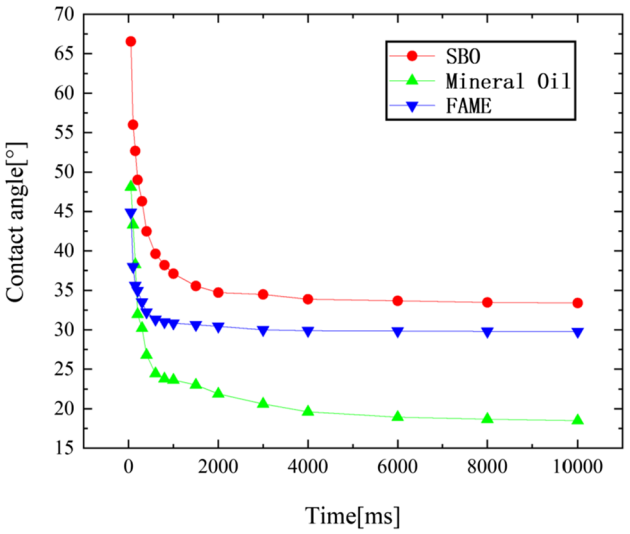

Fig. 7 The history of contact angle

scanning analysis (GC–MS) was performed to determine the specific chemical composition of the fatty acid methyl ester mixture (Fig. 2).

3.1.1 Proton nuclear magnetic resonance(H-NMR)

After the transesterification reaction, a small amount of the reaction product was taken for NMR hydrogen spectroscopy analysis, and the NMR hydrogen spectrum profile was obtained as shown in Fig. 3. The NMR hydrogen spectra of the reaction products (Fig. 3) were compared with the NMR hydrogen spectra of the untreated kitchen waste oil (Fig. 2). This was used to obtain the changes in the composition of the substances before and after the ester exchange reaction.

Figure 2 shows the H-NRM spectrum of the kitchen waste oil before the transesterification reaction. In the spectrum, the proton peaks at 5.3 ppm are the hydrogen atoms on the double carbons at the ends of the alkene bond, and the double peaks between 4.11–4.31 ppm are the – CH2 proton peaks in the glycerol molecule. At the right end of the spectrum, 1.29 ppm is the proton peak of the methylene group on the fatty acid chain and 0.88 ppm is the proton peak of the methyl group at the end of the carbon chain [28].

In the H-NRM profile of FAME, the glycerol -CH2 proton peak in the range of 4.11–4.31 ppm disappears completely and a completely new – OCH3 proton peak appears at 3.67 ppm compared to the H-NRM profile of the kitchen waste oil (Fig. 2). The proton peak at 2.33 ppm is that of the methylene adjacent to the carbonyl group. These changes indicate that the ester exchange reaction was successful in synthesizing high purity fatty acid methyl esters. The original fatty acid triglycerides in the kitchen waste oil were almost completely lost. The fatty acid attached to the methanol hydroxyl group resulted in a decrease in the electron density of methylene-CH2 in the carbon chain of the fatty acid. As a result, the proton peaks of methyl and methylene are chemically shifted and new proton peaks appear at 1.33 ppm and 0.93 ppm [29].

3.1.2 Gas chromatography–mass spectrometry(GC–MS)

The spectrum obtained from the gas chromatography–mass spectrometry analysis of the fatty acid methyl ester composition is shown in Fig. 4.

The peaks were characterized according to the NIST library and the relative fatty acid contents were calculated using the area normalization method. The fatty acid composition ratios of the mixtures were obtained as shown in Table 1.

3.2 Thermophysical properties and wetting kinetics

3.2.1 Thermophysical properties of quenchants

Table 2 shows the thermophysical properties of the three quenchants. The differences in density (at 20℃) and thermal

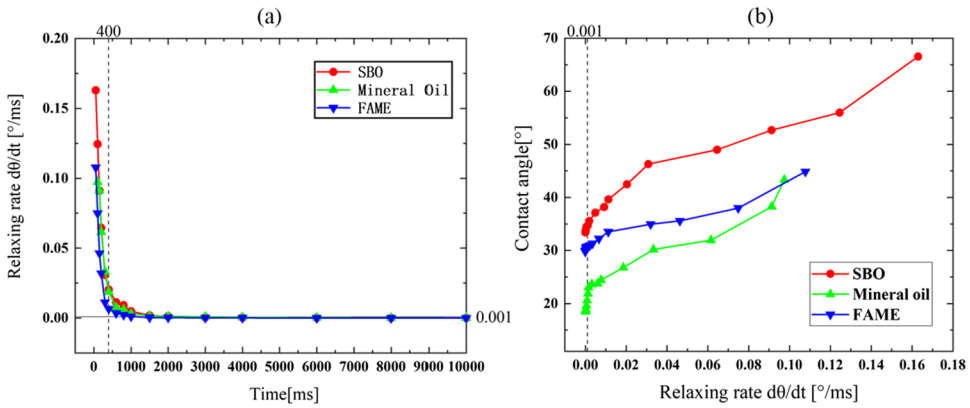

Fig. 8 The relaxing rate of contact angle. **a** Time (ms); **b** relaxing rate dθ/dt (°/ms)

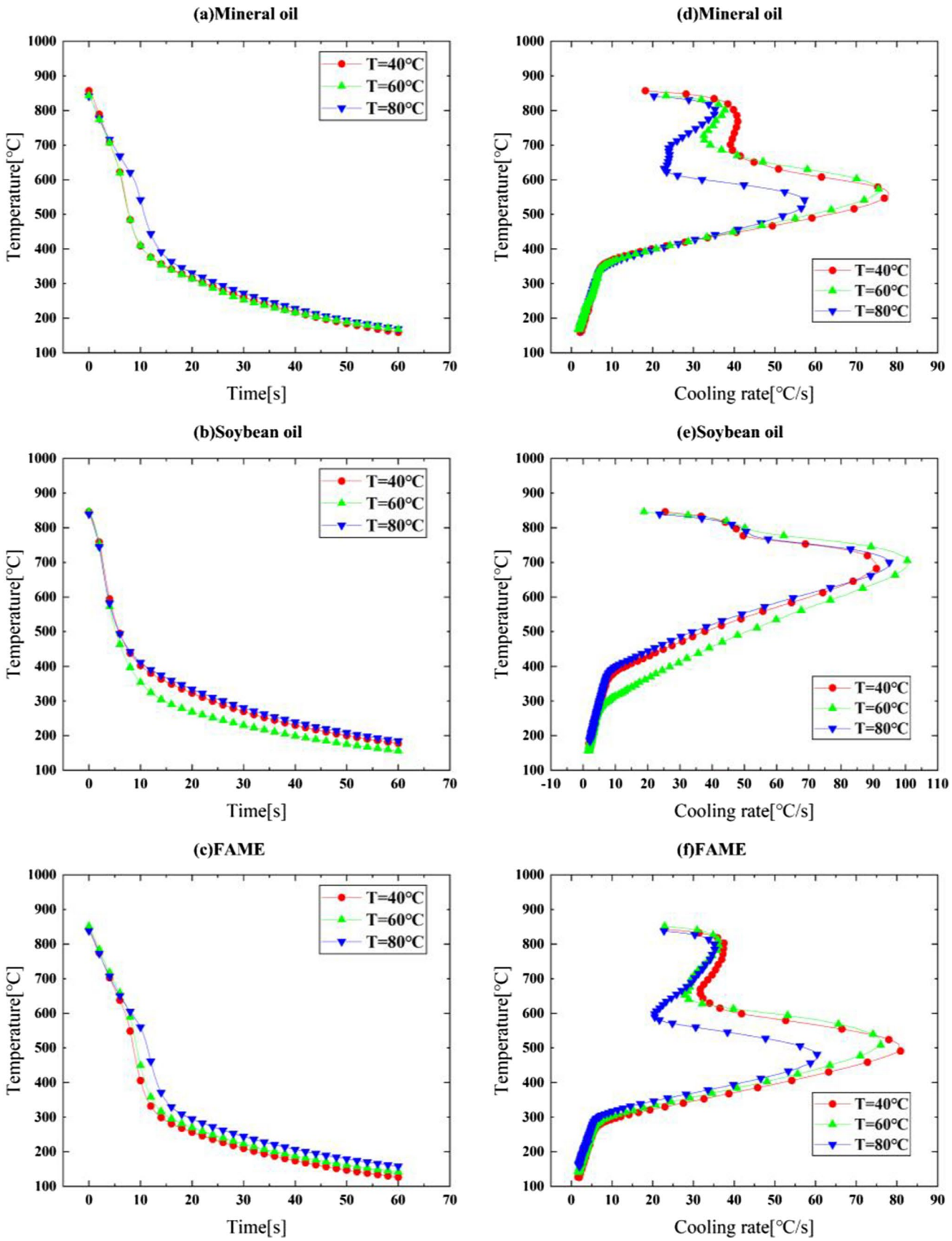

Fig. 9 Temperature evolution and absolute cooling rate curves registered during quenching of quench probe in **a**, **d** mineral oil; **b**, **e** soybean oil; and **c**, **f** FAME

Table 4 Summary of the cooling curve characteristics obtained for the specimens quenched in FAME, soybean and mineral oils (CR_{max}, maximum cooling rate (°C/s);T_{max}, temperature of CR_{max} (°C); CR300, cooling rate at 300 °C (°C/s); T600, time to reach 600 °C (s); T400, time to reach 400 °C (s); T200, time to reach 200 °C (s); F, FAME; S, soybean; and M, mineral oils; quenchant temperature presented in subscripts)

	M_{40}	M_{60}	M_{80}	S_{40}	S_{60}	S_{80}	F_{40}	F_{60}	F_{80}
T_{max}	559.7	572.6	537.3	718.8	696.7	700.2	510.9	521.0	476.4
CR_{max}	83.0	80.2	61.5	102.4	107.0	100.8	85.7	81.0	64.1
CR_{300}	6.1	7.6	7.4	6.2	8.3	5.6	12.3	9.8	7.1
T_{600}	6.3	6.3	8.7	3.4	3.7	3.7	7.1	7.8	8.2
T_{400}	10.4	10.5	13.6	8.7	7.9	11.0	10.1	10.9	13.2
T_{300}	22.6	22.1	24.9	19.0	14.6	26.0	13.9	15.5	19.2
T_{200}	45	45.7	48.2	41.8	39.8	53.2	34.5	38.2	42.2

conductivity between the three quench media are relatively small, with the relevant data for FAME being closer to that of mineral oil. The flash point data for soya oil is overwhelmingly superior, reflecting the potential of vegetable oils as quenching media. Compared to soya oil, FAME has a lower flash point temperature, but is still higher than that of common mineral oils. Quench media with high flash point temperatures have a wider process temperature range to choose from when quenching.

3.2.2 Viscosity of quenchants

The kinematic viscosity of the liquid reflects the flow of liquid, the friction between the molecules of the liquid. In general, the greater the relative molecular mass of a liquid, the higher its kinematic viscosity. Relative molecular mass is the main factor in determining the viscosity of a quenching medium. Table 3 and Fig. 5 show the trends in kinematic viscosity of the three quenchants at different temperatures. The kinematic viscosities of all three show a decreasing trend with increasing temperature. The trend for FAME is like that of 10# mineral oil.

In this experiment, the mineral oil used as the quenching medium was 10# mechanical oil, the main component of which was a saturated alkane with a carbon chain length of 10–20. The relative molecular mass of FAME is similar to that of 10# mechanical oil, so the kinematic viscosities of the two are also very similar. However, the kinematic viscosity of FAME is slightly higher than that of the mineral oil at the same temperature, probably due to the presence of unsaturated fatty acids in FAME. This slight difference will also be reflected in the subsequent cooling characteristics tests.

3.2.3 Wetting characteristics

Wetting occurs when the workpiece is immersed in the quenching medium. Generally, quenching oil in the workpiece surface contact angle size as a criterion for judging the wettability of quenching oil [30]. In general, when the quenching oil in the substrate material surface to form droplets of the wetting angle $\theta < 90°$, the quenching oil has a good wettability [31]. The better the wettability of the quench oil, the quench oil can be considered to be in full contact with the surface of the material, the easier it is to transfer heat from the surface of the material [32].

Figure 6 illustrates the diffusion of three types of quench media droplets onto the Inconel 600 material substrate as captured by the high-speed camera. Initially, the droplets contact the smooth material substrate surface to form semi-circular oil droplets [33]. The three-phase contact point at the edge of the droplet, at the point of contact with the substrate material and air, is referred to as the contact line front. At this point, a tangent to the circular profile of the droplet is made and the angle formed by this tangent to the substrate plane is the wetting or contact angle of the liquid [34].

As shown in Fig. 7, the contact angle formed by the oil droplets is large at the beginning of the contact. However, as time passes, the contact angle between the liquid and the substrate surface gradually decreases. The trend of contact angle change for the three oil droplets is basically the same, with the rate of contact decline being higher in the time period where the contact time is less than 400 ms. At the same time, the rate of change in contact angle slowed down sharply (Fig. 8a). After the contact time reached 400 ms, the change in contact angle gradually smoothed out. The higher viscosity oil droplets also show a faster rate of angular change. As shown in Fig. 8a and Fig. 8b, during the angular decrease in wetting angle, the rate of change shows a trend of soybean oil > methyl ester > mineral oil. In general, when the rate of change of the contact angle dθ/dt is less than 0.001°/ms, the angle is referred to as a stable contact angle or equilibrium contact angle. The equilibrium contact angles for soya oil, mineral oil, and FAME were 34.48°, 20.06°, and 30.64°.

Overall, comparison of the kinematic viscosity data for quench oils in 3.1.1 shows that there is a correlation between

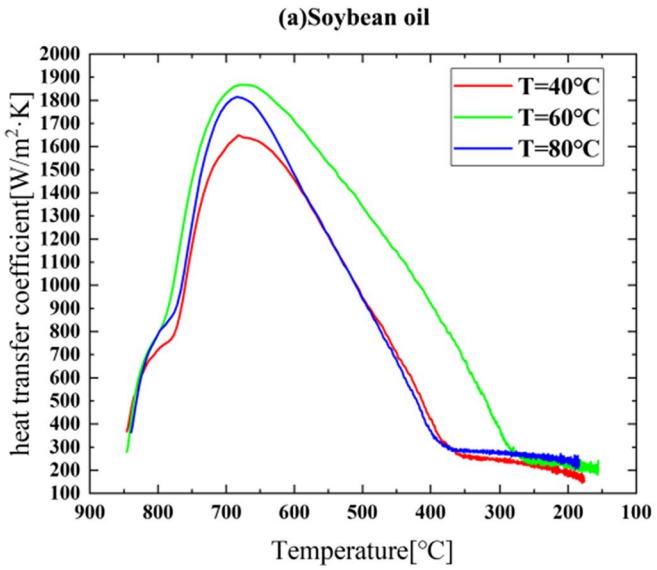
(a)Soybean oil
heat transfer coefficient[W/m²·K]
Temperature[°C]
T=40°C
T=60°C
T=80°C

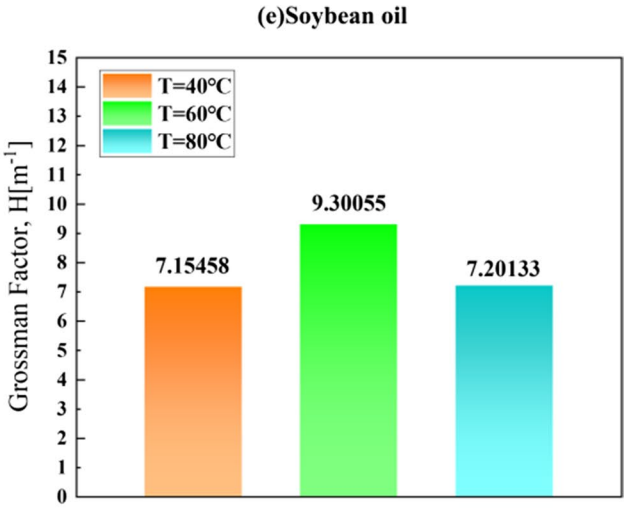
(e)Soybean oil
Grossman Factor, H[m⁻¹]
T=40°C
T=60°C
T=80°C
7.15458
9.30055
7.20133

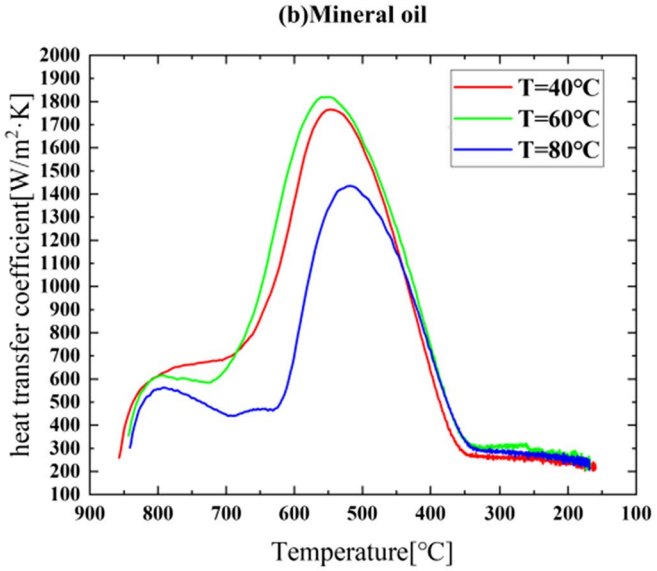
(b)Mineral oil
heat transfer coefficient[W/m²·K]
Temperature[°C]
T=40°C
T=60°C
T=80°C

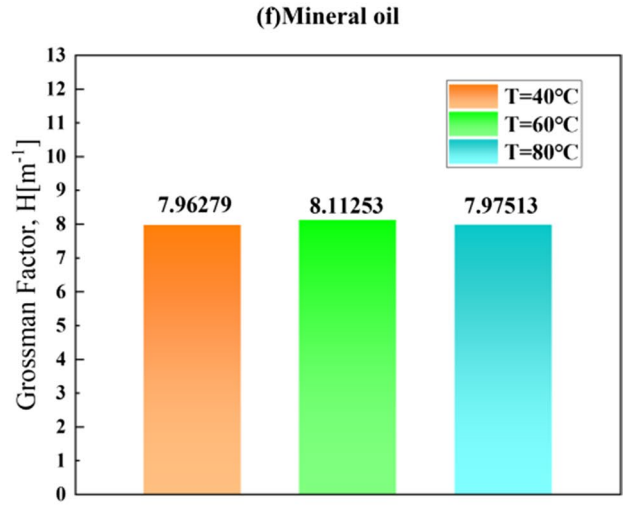
(f)Mineral oil
Grossman Factor, H[m⁻¹]
T=40°C
T=60°C
T=80°C
7.96279
8.11253
7.97513

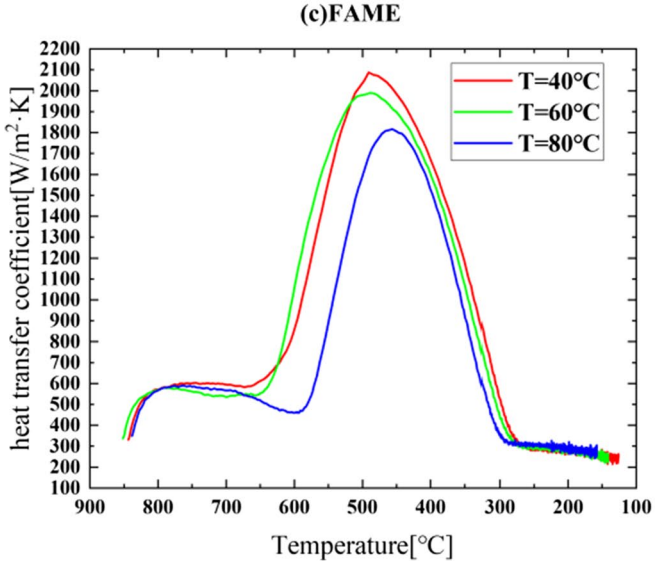
(c)FAME
heat transfer coefficient[W/m²·K]
Temperature[°C]
T=40°C
T=60°C
T=80°C

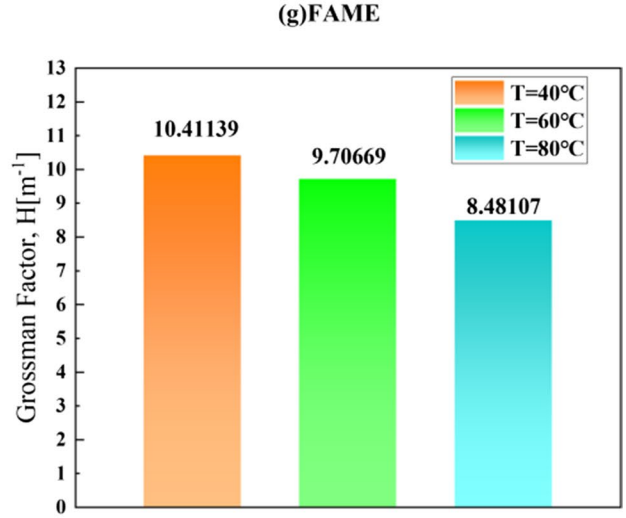
(g)FAME
Grossman Factor, H[m⁻¹]
T=40°C
T=60°C
T=80°C
10.41139
9.70669
8.48107

◂**Fig. 10** The heat transfer coefficient of quenching probe in **a** soybean oil, **b** FAME, and **c** mineral oil and Grossman factors *H* of **e** soybean oil, **f** FAME, and **g** mineral oil

the equilibrium contact angle size of a quench oil and its kinematic viscosity, with the higher the kinematic viscosity of the quench oil, the higher the equilibrium contact angle. Therefore, the ranking of excellent wettability shows mineral oil > methyl ester > soybean oil. Although the difference in kinematic viscosity index between FANE and mineral oil is smaller than the difference in equilibrium contact angle size between the two. This phenomenon is also present in the experimental phenomena for other vegetable oils. The reason for this phenomenon may be the presence of ester groups in fatty acid ester oils, which affects the wettability of the quench oil on the metal surface. The equilibrium contact angle size reflects to a certain extent the wettability of the quenching medium.

3.3 Cooling behavior of quenchants

In the cooling performance test, the heated nickel alloy probe is immersed in the quenchant for rapid cooling. A k-type thermocouple mounted at the center of the nickel alloy probe collects the temperature vs. time data and generates a temperature vs. time curve in the computer as shown in Fig. 9(a–c). After differentiation, the temperature vs. time curve is converted into a cooling rate-temperature curve for the probe surface temperature corresponding to the cooling rate (°C/s), as shown in Fig. 9(d–f). The data for the probe surface temperature cooling in different quench oils are shown in Table 4.

3.3.1 Cooling curves of quenchants

As the austenitising temperature of the workpiece is much higher than the boiling point of the vast majority of quenching media, the heat exchange between the workpiece and the media during cooling not only exists as thermal convection heat exchange, but also involves a variety of different heat exchange mechanisms [5, 35], corresponding to the different stages of the cooling rate trends.

The moment the workpiece is immersed in the quenchant, the quenchant rapidly vaporizes and forms a gas film covering the surface of the workpiece [36]. This phenomenon is known as the Leidenfrost effect. During this stage, the surface temperature of the workpiece cools at a low rate, creating a stable "cooling rate plateau." This stage is known as the vapor blanket stage. This is shown in Fig. 9(d) and Fig. 9(f).

And when the surface temperature of the workpiece drops, the liquid medium will escape in the form of many vapors' bubbles formed on the surface of the workpiece in the form of vaporization. At this point, the cooling of the workpiece enters the nucleate boiling stage. Finally, when the surface temperature of the workpiece drops further, the boiling bubbles will also disappear, and the cooling enters the final convection stage. The different stages have differential cooling rates, making the cooling process of the workpiece cooling rate in constant change.

Typically, the quenching medium in the vapor blanket stage has the worst heat transfer properties and the slowest cooling rate. During the nucleate boiling stage, the workpiece cools at a faster rate, with most of the quench process having a peak cooling rate during the nucleate boiling stage. When the convection stage is entered, the workpiece cooling rate decreases and gradually becomes smooth.

As shown in Fig. 9, the trend of the cooling curve for methyl ester is similar to that of the mineral oil cooling curve. Both quenching media undergo three cooling phases: vapor blanked stage, nucleate boiling stage, and convection stage. However, the cooling characteristics curve for soybean oil is unique in that the vapor blanket stage is extremely short and there is no "cold rate plateau" in the temperature cooling rate curve.

The cooling curve (temperature vs. time) data in Table 4 shows that the maximum cooling rates for all three quenching media were low. Soybean oil had the highest maximum cooling rate, with 102.4 °C/s, 107.0 °C/s, and 100.8 °C/s at 40 °C, 60 °C, and 80 °C. Furthermore, the surface temperature of the test probes was highest when soybean oil reached its maximum cooling rate compared to the other two types of quenching oils. Their temperatures were 718.8 °C, 696.7 °C, and 700.2 °C respectively. In contrast, the cooling curves for mineral oil and FAME were closer and the maximum cooling rates were very similar. The temperature at which the maximum cooling rate for both was 200 °C lower compared to soybean oil. The maximum cooling rates for mineral oil were 83.0 °C/s, 80.2 °C/s, and 61.5 °C/s at 40 °C, 60 °C, and 80 °C respectively, while the maximum cooling rates for FAME were 85.7 °C/s, 81.0 °C/s, and 64.1 °C/s at 40 °C, 60 °C, and 80 °C respectively.

Correspondingly, the soybean oil quenchant cooled the probe temperature to 600 °C in 3.4 s, 3.7 s, and 3.7 s at different oil bath temperatures. The 600 °C reach times for mineral oil were 6.3 s, 6.3 s, and 8.7 s. The cooling rate for FAME was lower in the high temperature stage and its 600 °C reach times were 7.1 s, 7.8 s, and 8.2 s. The cooling rate for FAME in the cooling rate in the high temperature range of 850–600 °C is essentially the same as that of mineral oil, and it is slightly less than mineral oil at lower oil bath temperatures.

The low temperature stage, where the surface temperature of the workpiece is below 300 °C, is the period

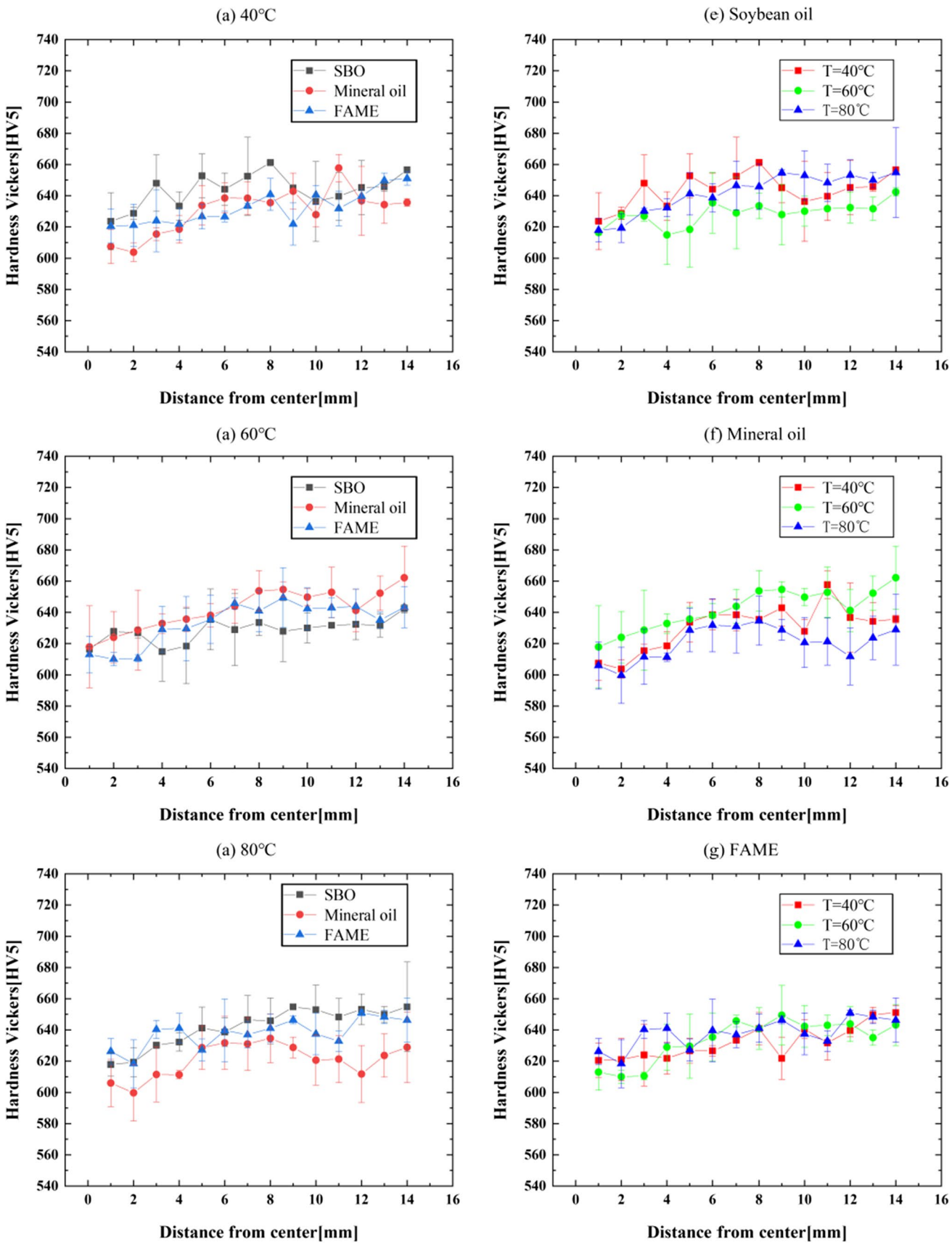

Fig. 11 Hardness gradient distribution curve

when the material undergoes martensitic transformation. The cooling rate should be kept as low as possible to avoid quenching cracks during the martensite generation process. Soybean oil has the lowest cooling rate at the beginning of the low temperature stage. Soybean oil in the workpiece has a temperature of 300 °C, and its three oil bath temperature cooling rate is 6.4 °C/s, 6.2 °C/s, and 8.3 °C/s. Mineral oil cooling rate is slightly higher, and its cooling rate is 6.1 °C/s, 7.6 °C/s, and 7.4 °C/s respectively. FAME has the highest CR300, with maximum cooling rates of 12.3 °C/s, 9.8 °C/s, and 7.1 °C/s for oil bath temperatures of 40 °C, 60 °C, and 80 °C, respectively. Mineral oil takes 22.4 s, 23.6 s, and 23.3 s respectively for the temperature interval from 300 to 200 °C, while FAME takes 20.6 s, 22.7 s, and 23 s for the temperature drop in this interval. Comparing the average cooling speed of FAME and mineral oil in the low temperature stage, we can see that there is no significant difference between the two. This is due to the fact that the low temperature cooling rate of FAME decreases more quickly when entering the low temperature phase compared to mineral oil. These characteristic manifests itself in the total time, making it take less time to cool down instead.

Comparing the cooling performance curves of soya oil, mineral oil, and FAME, we see a clear difference between their cooling behavior. The cooling curve of FAME is very similar to that of mineral oil, although the raw material composition of FAME is a fatty acid ester of vegetable oil. Clearly, the cooling behavior of a quenching medium is mainly determined by its physical properties, such as density, viscosity, wettability, and vapor pressure. Even though the chemical composition of mineral oil and FAME is different, their similar thermophysical properties allow them to exhibit similar cooling behavior. This phenomenon also suggests that in practical industrial production, fatty acid methyl esters prepared from gutter oil can be used as a base oil for quenching media instead of mineral oil.

3.3.2 Evaluation of quench severity

The quenching intensity of the quenching medium is characterized by the Grossmann quenching intensity value H [37]. The method for obtaining the Grossmann quenching intensity from the time temperature profile was proposed by grub as shown in Eq. (1).

$$H\left(m^{-1}\right) = \overline{h}/2\lambda \tag{1}$$

In Eq. (1), $\overline{h}$ is the average heat transfer coefficient of the probe in the heat transfer process. The evaluation of the heat transfer process on the surface of a quenched probe is generally based on the total set heat transfer method, which idealizes the temperature distribution on the surface of the probe as a uniform temperature distribution. During the quenching process, it is assumed that the heat loss of the probe temperature drop is considered as the heat transfer process of the internal energy loss of the probe [38]. The formula for calculating the internal energy loss of the probe is shown in Eq. (2).

$$Q = hA\left(T - T_0\right) = -C_p\rho V\left(\frac{dT}{dt}\right) \tag{2}$$

Q is the heat flow rate, W; h, heat transfer coefficient on the probe surface; W/m^2 K; A, the surface area of the probe, m^2; T, the temperature of the probe, K; T_0, the temperature of the quenchant, K; Cp, the specific heat of the probe material, J/kg K; q, the specific density of the probe material, kg/m^3; V, the volume of the probe, m^3; t, the time, s; (dTp/dt), the cooling rate of the probe. The heat transfer coefficient h can be calculated from Eq. (3).

$$h = C_p\rho\frac{V}{A}\left(\frac{dT/dt}{T - T_0}\right) \tag{3}$$

By calculating the cooling performance curves of the three quenching media (Fig. 9), the distribution of the heat transfer coefficients at different probe temperatures was obtained as shown in Fig. 10. The average heat transfer coefficient $\overline{h}$ of the quenching media at different temperatures between 850 and 200 °C was also estimated, and the Grossmann quenching intensity values H[m^{-1}] for different quenching media at different oil bath temperatures were calculated according to Eq. (1).

The trends in the distribution of heat flow density at different temperatures were generally consistent with those of the cooling rate. The peak heat transfer coefficients at the three oil bath temperatures for soybean oil were 1649.27 W/(m^2·K), 1866.87 W/(m^2·K), and 1815.20 W/(m^2·K), respectively. In contrast, the peak heat transfer coefficients for the three oil bath temperatures for FAME were 2087.77 W/(m^2·K), 1989.29 W/(m^2·K), and 1815.96917 W/(m^2·K). The peak heat transfer coefficients for mineral oil were 1765.90 W/(m^2·K), 1820.40 W/(m^2·K), and 1434.69 W/(m^2·K) respectively. Comparing the peak heat flow densities of the different quenching media, it can be seen that the actual peak heat transfer coefficients show differences in magnitude due to the different surface temperatures at which the respective peak cold rates are located. Although the peak cold rate is lower than that of soybean oil, the peak heat transfer coefficient of methyl ester is the largest of the three.

The quenching intensity value H reflects the overall cooling capacity of the quenching medium and its

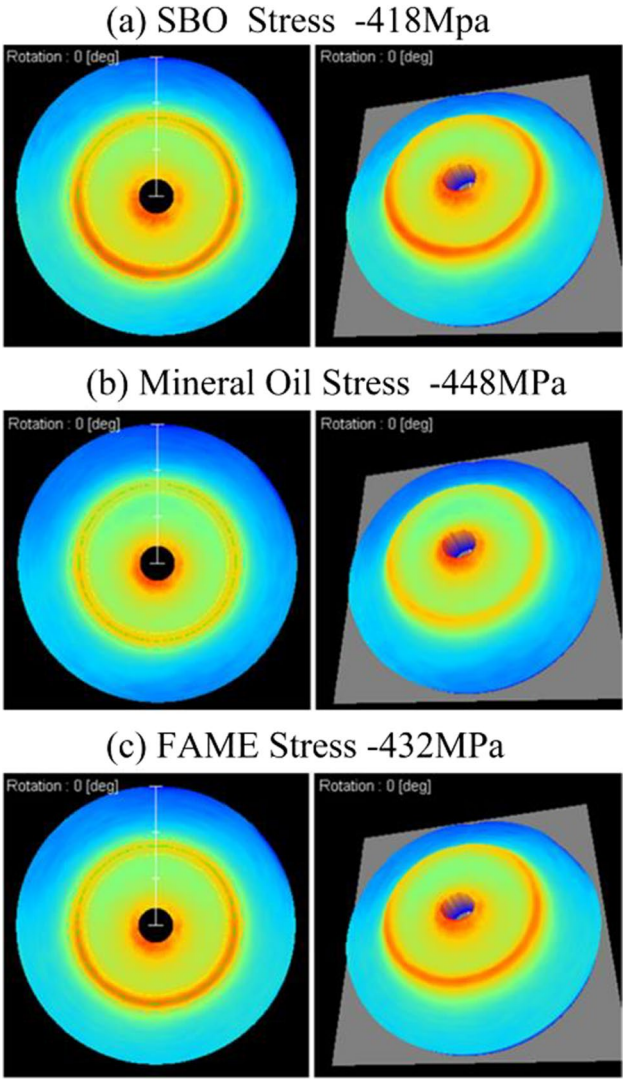

Fig. 12 Residual stress analysis performed on AISI 4340 specimens as a function of oil quenchant temperature. (**a**) SBO stress – 418 MPa; (**b**) mineral oil stress – 448 MPa; (**c**) FAME stress – 432 MPa

tendency to change. The *H* value for mineral oil is essentially constant for quench intensity *H* at different oil bath temperatures, while the quench intensity for the two fatty acid esters varies considerably depending on the oil bath temperature. Overall, methyl ester has the highest heat transfer coefficient as well as quenching intensity of the three quenchants, despite its lower maximum cooling rate. On balance, the quench cooling capacity of the methyl ester was stronger than the other two controls.

3.4 Hardness distributions

Quenching was carried out using AISI 4340 steel specimens in quenching oil at different oil bath temperatures and the quenched specimen sections were tested for microhardness along the radial direction. Microhardness gradient distribution curves were obtained as shown in Fig. 11(a-g). By comparing the hardness gradient distribution curves of the specimen sections under different quenching conditions, the correlation that exists between the phase change and the cooling curve during quenching was assessed. Figure 11(a-c) shows the hardness distribution curves for AISI 4340 steel specimens treated with different quenching oils under the same oil bath temperature conditions. Figure 11(e-g) shows the hardness distribution curves for AISI 4340 steel specimens treated with soybean oil, mineral oil, and FAME at different oil bath temperatures.

The hardness of the AISI 4340 steel specimens was approximately 280 HV prior to heat treatment and after quenching; all specimens showed a significant increase in hardness, with most of test points reaching over 600 HV. This indicates that the cooling rate of all three quenching oils reached the minimum cooling rate for martensitogenesis of AISI 4340 steel. Effective martensitic transformation occurred in the center and on the surface of the specimen material. From the hardness distribution gradient, all three quenching oils showed a gradual increase in the hardness gradient along the radial direction from the center to the edge of the workpiece. This reflects a positive correlation between hardness and cooling rate, with faster heat dissipation and higher microhardness near the surface of the specimen. At 40 °C and 60 °C, the hardened specimens in FAME and mineral oil each have a similar hardness distribution. Under 80 °C oil bath conditions, the hardness of the FAME quenched specimens was 20–30 HV higher than that of the mineral oil–quenched specimens, with a better hardening effect.

Subsequent X-ray diffraction residual stress tests on specimens quenched at 80 °C in an oil bath showed us more information. According to previous studies, the residual stress values of the quenched specimens showed a positive correlation with the CR300 of the quenching medium as well as the cooling rate at the low temperature stage. In the XRD residual stress test as shown in Fig. 12(a), the soybean oil quench experiment showed the lowest residual stress values. The FAME-quenched specimens, on the other hand, showed slightly lower residual stresses than the mineral oil specimens. This phenomenon is also consistent with the order of magnitude relationship between the three CR300s at 80 °C oil bath. At the higher temperature oil bath conditions, the FAME-quenched workpiece achieved the same hardening effect as the mineral oil quench, while having lower quench stresses.

4 Conclusion

The composition, wettability, thermophysical, and heat transfer properties and of FAME prepared from kitchen waste oil were investigated in this project. The fatty acid methyl ester was used as the quenching medium base oil for cooling rate testing, and mineral oil and soybean oil were set up as control groups to compare the performance differences between the three. Also, AISI 4340 steel was used as the specimen for quenching and the hardness distribution and residual stress magnitude of the samples were tested. The correlation between the cold speed curve and the cooling effect was analyzed. Based on the experimental studies, the following conclusions were obtained:

1. FAME made from gutter oil has a good heat transfer capacity as a quenching oil. Its maximum cooling rate was 85.7 °C/s, 81.0 °C/s, and 64.1 °C/s at 40 °C, 60 °C, and 80 °C oil bath temperatures, respectively.
2. The peak heat transfer coefficients for the three oil bath temperatures (40 °C, 60 °C, 80 °C) for FAME were 2087.77 W/(m^2·K), 1989.29 W/(m^2·K), and 1815.96917 W/(m^2·K). The quenching intensity *H* values for FAME were 10.41, 9.70, and 8.48 at 40 °C, 60 °C, and 80 °C in the oil bath respectively.
2. FAME has better wettability compared to soybean oil, indicating that esterification to reduce the average molecular weight treatment can enhance the wettability of fatty acid esters.
3. FAME also has a faster medium temperature cooling rate compared to mineral oil. In controlled quench tests, similar quench-hardening results were achieved, and FAME-quenched parts had lower residual stresses at the same oil bath temperature.
4. FAME is significantly less costly than soya oil and is more environmentally friendly than mineral oil due to its ease of degradation, bio-affinity, and low toxicity. It is also able to achieve the same hardening and quenching effect as soya oil. It has good potential for commercial application.

Author contribution Zongxiu Zhu: conceptualization, methodology, writing—original draft preparation, investigation; Weiyi Zhang: methodology, investigation; Dewen Zhang: software; Zhan Gao: software; Jiqiu Qi: conceptualization; Fuxiang Wei: validation; Qingkun Meng: validation; Yaojian Ren: investigation; Lichao Chai: resources; Zhi Sun: resources; Yanwei Sui: writing—review and editing, funding acquisition.

Funding This work was financially supported by the Fundamental Research Funds for the National Natural Science Foundation of China (no. 52171227 and 51871238); the Postdoctoral Research Funding Program of Jiangsu province (No.2021K043A); Xuzhou Science and Technology Project (No. KC21338); Key R&D Programs in Jiangsu Province (No. BE2021633); Fundamental Research Funds for the Central Universities (No. 2021ZDPY0221).

Declarations

Conflicts of interest There declare no competing interests.

References

1. Karmee SK (2016) Fuel not food-towards sustainable utilization of gutter oil. Biofuels 8:339–346. https://doi.org/10.1080/17597269.2016.1231952
2. Bernard A, Broeckaert F, De Poorter G, De Cock A, Hermans C, Saegerman C, Houins G (2002) The Belgian PCB/dioxin incident: analysis of the food chain contamination and health risk evaluation. Environ Res 88:1–18. https://doi.org/10.1006/enrs.2001.4274
3. Efsa SO (2008) Statement of EFSA on the risks for public health due to the presence of dioxins in pork from Ireland. EFSA J 6:911. https://doi.org/10.2903/j.efsa.2008.911
4. Koudil Z, Ikkene R, Mouzali M (2014) Cooling capacity optimization: calculation of hardening power of aqueous solution based on poly(N-vinyl-2-pyrrolidone). J Mater Eng Perform 23:551–559. https://doi.org/10.1007/s11665-013-0775-9
5. Edalatpour M, Cusumano DT, Nath S, Boreyko JB (2022) Three-phase Leidenfrost effect. Physical Review Fluids 7 https://doi.org/10.1103/PhysRevFluids.7.014004
6. Vilela Costa L, GonçalvesCarneiro JR, Pinto Coelho Catalão R, Ribas OK, Brito P (2014) Residual stress gradients in AISI 9254 steel springs submitted to shot peening and heat treatment for increased fatigue resistance. Advanced Materials Research 996:749–754. https://doi.org/10.4028/www.scientific.net/AMR.996.749
7. Ikkene R, Koudil Z, Mouzali M (2014) Cooling Characteristic of polymeric quenchant: calculation of HTC and prediction of microstructure and hardness. J Mater Eng Perform 23:3819–3830. https://doi.org/10.1007/s11665-014-1185-3
8. Chen X, Zhang L, Jie X, Li Y, Huang X (2017) Quenching characteristics of glycerol solution as a potential new quenchant. Int J Heat Mass Transf 109:209–214. https://doi.org/10.1016/j.ijheatmasstransfer.2017.02.013
9. Belinato G, Canale LCF, Totten GE, Canale L, Dean SW (2011) Effect of antioxidants on oxidative stability and quenching performance of soybean oil and palm oil quenchants. Journal of ASTM International 8 https://doi.org/10.1520/jai103376
10. Ramesh G, Prabhu KN (2014) Comparative study of wetting and cooling performance of polymer–salt hybrid quench medium with conventional quench media. Exp Heat Trans 28:464–492. https://doi.org/10.1080/08916152.2014.913088
11. Arularasan R, Babu K (2021) Thermally annealed biochar assisted nanofluid as quenchant on the mechanical and microstructure properties of AISI-1020 heat-treated steel—a cleaner production approach. Biomass Conversion Biorefinery. https://doi.org/10.1007/s13399-021-01737-x
12. Augustine Samuel KNP (2022) Residual stress and distortion during quench hardening of steels: a review. J Mater Eng Performance. https://doi.org/10.1007/s11665-022-06667-x
13. Thendral Thiyagu SPKJVT, Gurusamy P, Sathiyamoorthy V, Maridurai T, Arun Prakash VR (2021) Effect of cashew shell

biomass synthesized cardanol oil green compatibilizer on flexibility, barrier, thermal, and wettability of PLA/PBAT biocomposite films. Biomass Conversion Biorefinery 271:217–222. https://doi.org/10.1007/s13399-021-01941-9
14. Arun Prakasha RVVR (2019) Fabrication and characterization of echinoidea spike particles and kenaf natural fibre-reinforced Azadirachta-Indica blended epoxy multi-hybrid bio composite. Composites Part A-Appl Sci Manufactur 118:317–326. https://doi.org/10.1016/j.compositesa.2019.01.008
15. Ben Samuel SJJJ, Sivakumar K, Mayakannan AV, Arunprakash VR (2021) Visco-elastic, thermal, antimicrobial and dielectric behaviour of areca fibre-reinforced nano-silica and neem oil-toughened epoxy resin bio composite. SILICON 13:1703–1712. https://doi.org/10.1007/s12633-020-00569-0
16. Totten HMTGE, Lainer K (1999) Performance of vegetable oils as a cooling medium in comparison to a standard mineral oil. JMEPEG 8:409–416. https://doi.org/10.1361/105994999770346693
17. Sivriu AM, Sapunaru OV, Sterpu AE, Cioroiu Tirpan DR, Chis TV, Dobre T (2021) Thermal treatment under vacuum for obtaining a quenchant from rapeseed oil. Processes 9 https://doi.org/10.3390/pr9122189
18. Gu J, Xu J, Simencio Otero Rl, Viscaino JM, Canale LCF, Totten GE 2019 Heat transfer coefficients and quenching performance of vegetable oils, heat treat 2019: Proceedings from the 30th Heat Treating Society Conference and Exposition 272–278
19. MP Prathviraj, A Samuel, K Narayan Prabhu (2020) Reprocessed waste sunflower cooking oil as quenchant for heat treatment. Journal of Cleaner Production 269 https://doi.org/10.1016/j.jclepro.2020.122276
20. Brito P, Ramos PA, Resende LP, de Faria DA, Ribas OK (2019) Experimental investigation of cooling behavior and residual stresses for quenching with vegetable oils at different bath temperatures. J Clean Prod 216:230–238. https://doi.org/10.1016/j.jclepro.2019.01.194
21. Dodo RM, Ause T, Dauda ET, Shehu U, Gaminana JO, Popoola API, Mudiare E (2020) Mechanical properties and microstructures data of AISI 1070 steel quenched in epoxidized transesterified cottonseed oil. Data Brief 32:106100. https://doi.org/10.1016/j.dib.2020.106100
22. Said D, Belinato G, Sarmiento GS, Otero RLS, Totten GE, Gastón A, Canale LCF (2013) Comparison of oxidation stability and quenchant cooling curve performance of soybean oil and palm oil. J Mater Eng Perform 22:1929–1936. https://doi.org/10.1007/s11665-013-0560-9
23. Canale FMLD, Agustinho SCM, Totten GE, Farah AF (2005) Oxidation of vegetable oils and its impact on quenching performance. Mater Prod Technol 24:1–4. https://doi.org/10.1504/IJMPT.2005.007943
24. de Souza EC, Canale LCF, Sarmiento GS, Agaliotis E, Carrara JC, Schicchi DS, Totten GE (2013) Heat transfer properties of a series of oxidized and unoxidized vegetable oils in comparison with petroleum oil-based quenchants. J Mater Eng Perform 22:1871–1878. https://doi.org/10.1007/s11665-013-0514-2
25. Simencio Otero RL, Canale LCF, Said Schicchi D, Agaliotis E, Totten GE, Sánchez Sarmiento G (2013) Epoxidized soybean oil: evaluation of oxidative stabilization and metal quenching/heat transfer performance. J Mater Eng Perform 22:1937–1944. https://doi.org/10.1007/s11665-013-0546-7
26. Dodo RM, Ause T, Dauda ET, Shehu U, Popoola API (2019) Multi-response optimization of transesterification parameters of mahogany seed oil using grey relational analysis in Taguchi method for quenching application. Heliyon 5:e02167. https://doi.org/10.1016/j.heliyon.2019.e02167
27. Samuel A, Prabhu KN (2022) Assessment of Heat transfer characteristics of transesterified waste sunflower cooking oil blends for quench hardening. J Mater Eng Perform. https://doi.org/10.1007/s11665-022-06668-w
28. Flores IS, Godinho MS, de Oliveira AE, Alcantara GB, Monteiro MR, Menezes SMC, Lião LM (2012) Discrimination of biodiesel blends with 1H NMR spectroscopy and principal component analyses. Fuel 99:40–44. https://doi.org/10.1016/j.fuel.2012.04.025
29. de Jesus MDPM, de Melo LN, da Silva JPV, Crispim AC, Figueiredo IM, Bortoluzzi JH, Meneghetti SMP (2015) Evaluation of proton nuclear magnetic resonance spectroscopy for determining the yield of fatty acid ethyl esters obtained by transesterification. Energy Fuels 29:7343–7349
30. Prabhu KN, Fernades P, Kumar G (2009) Effect of substrate surface roughness on wetting behaviour of vegetable oils. Mater Des 30:297–305. https://doi.org/10.1016/j.matdes.2008.04.067
31. Ramesh G, Prabhu KN (2014) Wetting kinetics, kinematics and heat transfer characteristics of pongamia pinnata vegetable oil for industrial heat treatment. Appl Therm Eng 65:433–446. https://doi.org/10.1016/j.applthermaleng.2014.01.011
32. Ramesh G, Prabhu KN (2014) Wetting and cooling performance of mineral oils for quench heat treatment of steels. ISIJ Int 54:1426–1435. https://doi.org/10.2355/isijinternational.54.1426
33. Biance Anne Laure CF, Clanet C, Lagubeau G, Quéré D (2006) On the elasticity of an inertial liquid shock. J Fluid Mech 554:47. https://doi.org/10.1017/S0022112006009189
34. Fernandes P, Prabhu KN (2008) Comparative study of heat transfer and wetting behaviour of conventional and bioquenchants for industrial heat treatment. Int J Heat Mass Transf 51:526–538. https://doi.org/10.1016/j.ijheatmasstransfer.2007.05.018
35. Bernardin MIJD (1999) The Leidenfrost point: experimental study and assessment of existing models. J Heat Transfer 121:894–903. https://doi.org/10.1115/1.2826080
36. Biance CCAL, Quere D (2003) Leidenfrost drops. Phys Fluids 15:1632–1637. https://doi.org/10.1063/1.1572161
37. Prabhu KN, Ali I (2014) Comparison of Grossmann and lumped heat capacitance methods for assessment of heat transfer characteristics of quench media. Int Heat Treatment Surface Eng 5:41–46. https://doi.org/10.1179/174951411x12956208225140
38. Prabhu KN, Fernades P (2007) Nanoquenchants for industrial heat treatment. J Mater Eng Perform 17:101–103. https://doi.org/10.1007/s11665-007-9124-1